Evaluation of Specific Binding of [11C]RTI-97 to KOR by Autoradiog-raphy and PET Imaging in Rat

Fabien Fillesoye, Méziane Ibazizene, Nicolas Marie, Florence Noble, Cécile Perrio

Evaluation of Specific Binding of [^{11}C]RTI-97 to KOR by Autoradiography and PET Imaging in Rat

Fabien Fillesoye,[1] Méziane Ibazizène,[1] Nicolas Marie,[2] Florence Noble[2] and Cécile Perrio[1,*]

[1] Normandie Univ, UNICAEN, CEA, CNRS, UMR 6030, LDM-TEP, Cyceron, Boulevard Henri Becquerel, 14074 Caen, France

[2] Université de Paris, CNRS, ERL 3649, Inserm, UMR-S 1124, Pharmacologie et thérapies des addictions, 75006 Paris, France

ABSTRACT: Kappa opioid receptor (KOR) PET imaging remains attractive to understand the role of KOR in health and diseases, and to help the development of drugs especially for psychiatric disorders such as depression, anxiety and addiction. The potent and selective KOR antagonist RTI-97 labelled with carbon-11 was previously demonstrated to display specific KOR binding in mouse brain by *ex vivo* autoradiography studies. Herein, we evaluated [^{11}C]RTI-97 in rat by *in vitro* autoradiography and by *in vivo* PET imaging. The radiosynthesis of [^{11}C]RTI-97 was optimized to obtain high molar activities. Despite a low cerebral uptake, the overall results showed an heterogeneous repartition and specific KOR binding of [^{11}C]RTI-97 in brain, and a high and specific accumulation of [^{11}C]RTI-97 in pituitary in accordance with KOR expression.

KEYWORDS: Kappa opioid receptor, RTI-97, JDTic, carbon-11, autoradiography, positron emission tomography

Kappa opioid receptors (KORs) are known to play an important role in many physiological and pathological functions including immunomodulation, mood control, sensation of pain, anxiety, depression, drug abuse and psychiatric disorders.[1-4] They belong to G-protein-coupled receptor family and are the most abundant ORs in the human brain.[5] Although homology with MOR and DOR subtypes, KORs display a unique pharmacology with aversive effects produced by KOR agonists whereas MOR and DOR agonists are rewarding and reinforcing.[6] Potent KOR antagonists such as JDTic have been proposed as chemotherapy for cocaine, morphine and nicotine addiction as well as alcohol seeking.[7-11] As a result, efforts have been made to develop KOR PET imaging in order to better understand *in vivo* KOR pharmacology, to measure the KORs density, to investigate disease states and to evaluate new therapeutics.[12-13] The past decades have seen progress in the validation of KORs radioligands (Figure 1). Among them, [^{11}C]GR103545, [^{11}C]EKAP and [^{11}C]LY2795050 have been assessed in clinical trials. [^{11}C]GR103545 displayed slow binding kinetics and ultra-potency leading to risk of side effects such as dysphoria, sedation and psychosis due to its KOR agonist property.[14-15] The novel KOR agonist [^{11}C]EKAP was recently reported to display faster tissue kinetics than [^{11}C]GR103545 in test-retest reproducibility studies.[16-18] [^{11}C]LY2795050, identified as a KOR antagonist with short term effects, was shown to possess favorable brain uptake, pharmacokinetic properties and binding profiles but poor stability and moderate KOR selectivity.[19-24] The analogue [^{11}C]/[^{18}F]LY2459989 recently evaluated in non-human primates was suggested to display a similar *in vivo* behavior.[25-26] Thus, characterization of KOR radiopharmaceuticals with antagonism properties and high target specificity is still desirable.[27]

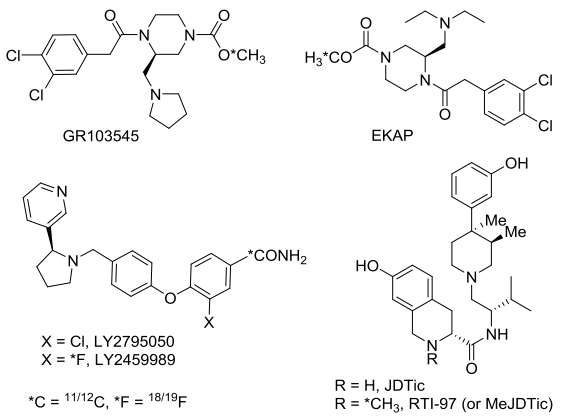

Figure 1. Structure of main KOR PET radioligands and JDTic derivatives.

Few years ago, we developed KOR radiotracers derived from JDTic [(3*R*)-7-hydroxy-N-((1*S*)-1-{[(3*R*,4*R*)4-(3-hydroxyphenyl)-3,4-dimethyl-1-piperidinyl]methyl}-2methylpropyl)-1,2,3,4-tetrahydro-3-isoquinolinecarboxamide] established as the most potent and selective KOR antagonist reported so far (Figure 1).[28-29] Among them, the *N*-[^{11}C]- methylated derivative [^{11}C]RTI-97 (or [^{11}C]RTI-5989-97, [^{11}C]-MeJDTic, (3*S*)-7-hydroxy-N-((1*S*)-1{[(3*R*,4*R*)-4-(3-hydroxyphenyl)-3,4-dimethyl-1-piperidinyl]methyl}-2-methylpropyl)-2-[^{11}C]methyl-1,2,3,4-tetrahydro-3-isoquinolinecarboxamide) was reported to exhibit a high specific binding to KOR in brain by *ex vivo* studies in mouse using competition and counting method.[28] RTI-97 was also reported to display advantageous pharmacological properties compared to JDTic. *In vitro* experiments from rodent

brain tissues [RTI-97: K_i (KOR) = 0.053 ± 0.03 nM, K_i (MOR) / K_i (KOR) = 700, K_i (DOR) / K_i (KOR) = 1162; JDTic: K_i (KOR) = 0.32 ± 0.05 nM, K_i (MOR) / K_i (KOR) = 12, K_i (DOR) / K_i (KOR) = 940] and human cloned receptors [RTI-97: K_i (KOR) = 1.01 ± 0.14 nM, K_i (MOR) / K_i (KOR) = 8.8, K_i (DOR) / K_i (KOR) = 117; JDTic: K_i (KOR) = 0.41 ± 0.10 nM; K_i (MOR) / K_i (KOR) = 2.3, K_i (DOR) / K_i (KOR) = 72] revealed that RTI-97 was more potent and selective than JDTic.[30] RTI-97 was also found to have a shorter duration of antagonism than JDTic in models of analgesia in mouse and in diuresis in rat, suggesting that pharmacokinetics would remain appropriate for imaging studies.[31] The long duration of action of JDTic and its derivatives, producing measurable antagonism for several weeks at minimally-effective doses, raised questions of mechanism, especially since brain penetration was low and clearance from plasma was rapid.[32] Lysosomes sequestration was proposed as explanation for JDTic brain persistence. However, such a hypothesis would lead to non-displaceable KOR binding, which was not in accordance with the previously cited [^{11}C]RTI-97 evaluation.[28] Thus, the overall findings prompted us to further investigate KOR binding properties of [^{11}C]RTI-97. Here, we report results for KOR specificity of [^{11}C]RTI-97 by *in vitro* autoradiography, *in vivo* PET imaging and *ex vivo* experiments in rats.

First of all, we revisited the radiosynthesis of [^{11}C]RTI-97 in order to obtain high molar activities. The radiolabeling was realized by ^{11}C-methylation of JDTic with [^{11}C]-methyl triflate obtained from $^{11}CH_4$ instead of $^{11}CO_2$ (Figure 2). [^{11}C]RTI-97 was purified and isolated by normal phase HPLC, then concentrated to dryness and formulated. This method was advantageous for time saving reasons (See Supporting Information). The overall production was performed on a commercial automated carbon-11 synthesis unit (TRACERlab FX MeI GE Healthcare). Ready to use [^{11}C]RTI-97 was obtained within 33 min from end of bombardment in 11-16% radiochemical yield (not decay corrected and relative to $^{11}CH_4$) with > 99% radiochemical and chemical purities and 111-259 GBq/µmol molar activities. Molar activities were 50-100 times higher than those obtained according to previously reported procedure (1.4-4.5 GBq/µmol).[28]

In vitro experiments were performed on healthy male Wistar rat brain slices with the radiotracer alone (baseline conditions) and with the addition of a large excess (x 2500) of naloxone, a non-selective OR antagonist, or U-50,488, a selective KOR agonist (blocking conditions) for the determination of [^{11}C]RTI-97 binding selectivity. All experiments were performed in triplicate with three different productions of [^{11}C]RTI-97. Autoradiography images revealed that the radioactivity was distributed heterogeneously over brain sections under baseline conditions and that radioactivity levels were significantly reduced under blocking conditions (Figure 3, Table 1). Under baseline conditions, the highest concentration of [^{11}C]RTI-97 was found in OT (olfactory tubercle), TH (thalamus), SC (superior colliculi) and CPU (caudate-putamen), with radioactivity ratios relative to CB (cerebellum) known to be poor in KORs reaching 1.5-1.7. Less binding was observed in ACB (nucleus accumbens), SNR (substantia nigra), CTX (cortex), HIP (hippocampus) and HY (hypothalamus), corresponding to radioactivity ratios relative to CB in the 1.4-1.2 range; and the lowest radioactivity levels were measured in CC (corpus callosum), AMY (amygdala) and CB as expected. This distribution was in accordance with KOR expression in rat brain regions.[33-34] In the competition studies using either naloxone or U-50,488, [^{11}C]RTI-97 binding was significantly reduced in all cerebral regions except CC and CB. Binding inhibition rates were in the 30-50% range in KOR expressing regions, while they were below 20% in KOR devoided structures such as CC and CB. These results indicated [^{11}C]RTI-97 binding specificity. Globally, naloxone and U-50,488 displayed a similar inhibition effect in [^{11}C]RTI-97 binding. The absence of a significant difference between naloxone and U-50,488 was in agreement with the specificity of [^{11}C]RTI-97 for KOR.

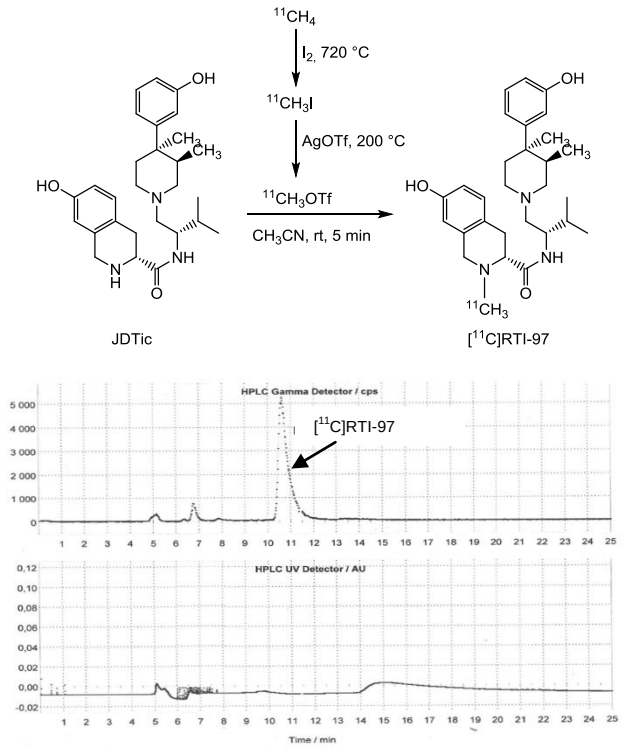

Figure 2. Radiosynthesis scheme of [^{11}C]RTI-97 from cyclotron produced [^{11}C]CH_4 (A) with representative semi-preparative HPLC (high performance liquid chromatography) chromatogram at the end of the radiosynthesis for the purification and isolation of [^{11}C]RTI-97 (B).

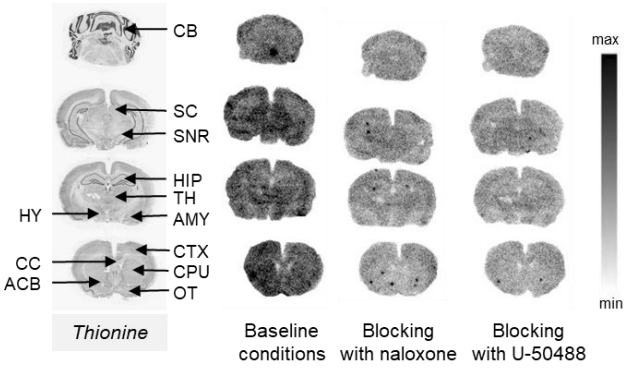

Figure 3. Representative autoradiography images of coronal brain sections after incubation with [^{11}C]RTI-97 (0.7 ± 0.2 GBq/L, *i.e.* 4.3 ± 0.8 nM; baseline conditions) or after co-incubation of [^{11}C]RTI-97 with naloxone (10 µM) or U-50,488

(10 μM) (blocking conditions). Tissue sections were counter-stained with thionine for brain structure identification.

Table 1. Brain structure (BS) distribution of radioactivity after incubation of rat brain slides with [^{11}C]RTI-97

Brain structure (BS)[a]	Radioactivity (10^3xDLU/mm^2 ± SEM)			BS/CB ratio[d] (baseline)	Binding inhibition (%)[e]	
	Baseline Conditions[b]	blocking with naloxone[c]	blocking with U50,488[c]		naloxone	U50,488
OT	8.07 ± 0.27	3.54 ± 0.70	3.10 ± 0.55	1.7 ± 0.6	47	43
TH	7.98 ± 0.18	4.97 ± 0.57	4.26 ± 0.13	1.6 ± 0.4	34	31
SC	7.79 ± 1.71	4.80 ± 0.47	3.94 ± 0.18	1.6 ± 0.4	35	35
CPU	7.62 ± 1.09	4.87 ± 1.03	3.28 ± 0.24	1.5 ± 0.3	37	49
ACB	6.86 ± 0.81	4.59 ± 0.83	2.98 ± 0.35	1.4 ± 0.3	33	51
SNR	6.79 ± 1.55	4.97 ± 0.40	3.86 ± 0.53	1.4 ± 0.1	20	27
CTX	6.41 ± 0.72	4.29 ± 0.94	3.57 ± 0.16	1.3 ± 0.2	32	38
HIP	6.29 ± 0.93	4.01 ± 0.56	3.51 ± 0.33	1.2 ± 0.2	35	34
HY	5.68 ± 1.08	4.14 ± 0.63	3.08 ± 0.54	1.2 ± 0.3	26	32
CC	5.67 ± 0.70	4.67 ± 0.63	4.03 ± 0.22	1.1 ± 0.1	18	22
AMY	5.31 ± 0.71	3.49 ± 0.59	2.56 ± 0.31	1.1 ± 0.2	35	44
CB	5.23 ± 0.91	5.11 ± 0.94	4.39 ± 0.67	1.0 ± 0.1	3	17

[a] BS are listed by decreasing radioactivity level. [b] Incubation of [^{11}C]RTI-97 (0.7 ± 0.2 GBq/L, *i.e.* 4.3 ± 0.8 nM) alone. [c] Co-incubation of [^{11}C]RTI-97 (0.7 ± 0.2 GBq/L, *i.e.* 4.3 ± 0.8 nM) with naloxone (10 μM) or U50,488 (10 μM). [d] BS/CB ratios calculated from values obtained under baseline conditions. [e] Calculated from values obtained under baseline conditions and blocking experiments with naloxone or U50,488 (significant inhibition > 30%).

The *in vivo* specific binding of [^{11}C]RTI-97 was then assessed by *in vivo* PET/CT imaging in healthy male Wistar rats. Rats were injected (iv, tail vein) with 34.2±8.0 MBq of [^{11}C]RTI-97 (corresponding to 0.2 to 12.1 μg/kg of RTI), and dynamic PET imaging was acquired over 30 min. In competition experiments, rats received naloxone or U-50,488 (1 mg/kg, iv, tail vein) 10 min prior injection of [^{11}C]RTI-97, or JDTic (10 mg/kg, ip) 30 min prior injection of [^{11}C]RTI-97. The use of different blockers was important as discrepancies in KOR radioligand binding has previously been revealed.[35]

PET Images under baseline conditions (injection of only [^{11}C]RTI-97) showed that brain uptake of [^{11}C]RTI-97 was very low, and that [^{11}C]RTI-97 accumulated in pituitary gland (Figure 4). Thus, time-activity curves (TACs) were extracted for whole brain, pituitary gland and muscle as reference. [^{11}C]RTI-97 uptake in pituitary gland was rapid with the maximum peak SUV values of about 1.6 reached from 3.5 min post-injection. These values remained constant until the end of 30 min acquisition, and they were 4 times higher than the SUV values for muscle uptake. TAC for muscle uptake displayed a similar profile of that for pituitary gland but with a lesser magnitude as the maximum peak SUV value also reached at 3.5 min was only 0.4. For pituitary gland and muscle, no wash out was observed during acquisition time. Uptake in brain was lower than in muscle with SUV values that did not exceed 0.4 at 1 min, and decreased to 0.2 to stay stable from 3 to 30 min.

For competition studies, TACs were determined for whole brain, pituitary gland and muscle by pooling all data obtained with naloxone, U-50,488 and JDTic. The pre-injection of the blockers had significant influence on [^{11}C]RTI-97 uptake in pituitary gland with SUV values of about 1.15 during the 3.5-30 min plateau, corresponding to 30% inhibition rate. In contrast, no difference between baseline and blocking conditions was observed in muscle and whole brain. As remark, the low radioactivity levels in brain were not appropriate to detect any significant inhibition.

In order to refine and complete the *in vivo* results, we undertook *ex vivo* experiments. Animals were euthanized at the end of the PET imaging session for brain and cerebral regions dissection and radioactivity counting, and also for evaluation of [^{11}C]RTI-97 stability in blood (Table 2). *Ex vivo* data were expressed as uptake index to correct for differences in animal body weight and injected dose (see Supporting Information). Radioactivity amounts in blood corresponding to uptake index of 0.25-0.33, were similar under baseline and blocker pre-injection conditions, confirming that the pharmacokinetics of [^{11}C]RTI-97 was not modified by the blockers. Moreover, HPLC analyses revealed that more than half of [^{11}C]RTI-97 was recovered intact in the circulation, and radiometabolites were found to be more polar than [^{11}C]RTI-97 and not to cross the BBB. These findings were in accordance with our previously reported studies carried out in mouse.[28]

As expected following PET imaging results, [^{11}C]RTI-97 concentration was high in pituitary gland with an uptake index reaching around 8 under baseline conditions. The uptake index decreased to 5.6 under blocking conditions with naloxone and U-50,488 as blockers, corresponding to around 30% inhibition, and dropped to 4.6 using JDTic, leading to inhibition rate of 43%. The inhibition rate was found to be significantly higher with JDTic than with naloxone and U-50,488. This difference could not be shown from PET imaging data due to a lack of sensibility compared to counting measurement, but globally the overall *ex vivo* results were of the same magnitude as those *in vivo*.

The radioactivity level for half brain remained very low with uptake index of 0.5-0.6 under both baseline and blocking conditions, value in the same order than that for CB. Once again, these results are in accordance with the low brain penetration determined by PET imaging. Interestingly, data for cerebral sub-structures displayed a significant heterogeneous radioactivity repartition despite the low radioactivity levels. Under baseline conditions, [^{11}C]RTI-97 uptake was high in HY and OT with radioactivity ratios relative to CB of 3.70 and

2.09 respectively, and it was lower in CPU, HIP and CTX with radioactivity ratios relative to CB ranging from 1.61 to 1.31. Radioactivity levels in TH were similar to that in CB. In HY and OT, 40% of [^{11}C]RTI-97 uptake was inhibited by pre-injection of U50,488. These inhibition results are coherent with those obtained by autoradiography (Table 1). The uptake inhibition in HY and OT was lower with naloxone and JDTic as blockers. In contrast, naloxone and JDTic lead to 28-37% of [^{11}C]RTI-97 binding inhibition in CPU whereas no effect was observed with U50,488. Inhibition by naloxone, U50,488 and JDTic below 25% was not significant in the other brain regions.

Figure 4. Representative axial and sagittal plans of fusion PET/CT (up), CT (middle) and PET (down) images with [^{11}C]RTI-97 under baseline (A) and blocking (B, using JDTic as blocker) conditions. Time-activity curves (TACs; SUV: standardized uptake value) of [^{11}C]RTI-97 obtained for pituitary (blue, * for $p < 0.05$), muscle (green) and whole brain (red) under baseline (solid lines, n = 4) and blocking (dotted lines, taken in account all results with naloxone (n = 5), U-50,488 (n = 5) and JDTic (n = 6) as blockers) conditions (C). Data were reported as mean values ± standard error of the mean (SEM).

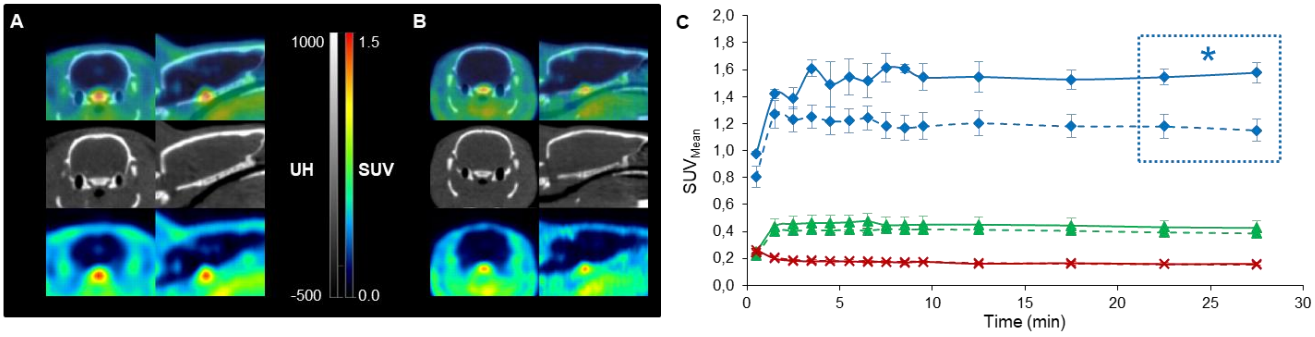

Table 2. Radioactivity distribution 30 min post-injection determined by counting after dissection

Tissue or BS	Uptake index (± SEM)				BS/CB ratio (baseline)	Uptake inhibition (%)[d]		
	baseline conditions	blocking with naloxone[a]	blocking with U50,488[b]	blocking with JDTic[c]		naloxone	U50,488	JDTic
Blood	0.25 ± 0.04	0.33 ± 0.09	0.24 ± 0.03	0.27 ± 0.04	*na*[e]	*na*[e]	*na*[e]	*na*[e]
Pituitary	8.06 ± 0.28	5.58 ± 0.48	5.61 ± 0.19	4.59 ± 0.67	*na*[e]	31	30	43
½ Brain	0.06 ± 0.01	0.05 ± 0.01	0.05 ± 0.01	0.06 ± 0.01	*na*[e]	-	-	-
HY	0.23 ± 0.07	0.17 ± 0.02	0.13 ± 0.02	0.17 ± 0.02	3.70 ± 1.31	-	43	-
OT	0.15 ± 0.03	0.17 ± 0.08	0.09 ± 0.01	0.13 ± 0.02	2.09 ± 0.30	-	40	-
CPU	0.12 ± 0.04	0.08 ± 0.01	0.13 ± 0.04	0.09 ± 0.01	1.61 ± 0.23	37	-	-
HIP	0.10 ± 0.01	0.09 ± 0.02	0.10 ± 0.01	0.10 ± 0.02	1.59 ± 0.39	-	-	-
CTX	0.09 ± 0.01	0.11 ± 0.05	0.08 ± 0.01	0.09 ± 0.01	1.31 ± 0.30	-	-	-
TH	0.08 ± 0.02	0.11 ± 0.06	0.06 ± 0.01	0.06 ± 0.01	1.11 ± 0.31	-	-	-
CB	0.07 ± 0.02	0.06 ± 0.01	0.07 ± 0.01	0.06 ± 0.01	1.00 ± 0.01	-	-	-

[a] Pre-injection of naloxone (1 mg/kg; iv; 10 min). [b] Pre-injection of U-50,488 (1 mg/kg; iv; 10 min). [c] Pre-injection of JDTic (10 mg/kg; ip; 30 min). [d] Only values for significant inhibition ($P < 0.041$). [e] Not applicable.

In summary, we have successfully developed the radiosynthesis of [^{11}C]RTI-97 with high molar activities. *In vitro* autoradiography studies demonstrated KOR specific binding in rat brain in accordance with KOR cerebral distribution. *In vivo* PET imaging and *ex vivo* studies in rats revealed a low brain penetration but a high uptake of [^{11}C]RTI-97 in pituitary. It has been largely shown that the implication of the KOR system in several physiopathological states such as addiction, stress and anxiety-related behaviors was related to the modulation of the hypothalamic–pituitary–adrenal (HPA) axis.[36-37] It was also well established that pituitary gland displayed high density of KORs.[38] MORs have also been found to be expressed but not DORs. Thus, the high accumulation of [^{11}C]RTI-97 in pituitary was expected, especially since this brain region was not protected by the blood-brain barrier (BBB). However, a non-specific entry could occur due to the significant vascularization and to hydrophobic properties of RTI-97. Both *in vivo* and *ex vivo* data demonstrated a significant [^{11}C]RTI-97 binding inhibition in pituitary by either naloxone, U-50,488 and JDTic. The higher inhibition effect measured in *ex vivo* studies using JDTic was also consistent with a higher affinity and specificity of JDTic for KORs compared to naloxone and U-50,488, and also confirmed [^{11}C]RTI-97 specific KOR binding. The high uptake and specific binding of [^{11}C]RTI-97 in pituitary was also nicely correlated to the significant concentration and specific binding revealed in HY by *ex vivo* experiments, according to the known KOR enriched expression in these two strongly attached structures.

These results may raise the question of whether KOR pituitary binding may be related to centrally mediated effects induced by RTI-97 and drugs from the same class of compounds.

To our knowledge, binding in pituitary was poorly investigated in the evaluation of KOR PET radiotracers, and the consideration of this structure may be underestimated. [^{3}H]Cyclofoxy, a ligand with high affinity for both MOR and KOR, was shown to label pituitary in *ex vivo* autoradiography studies.[39] A decreased binding of non-selective OR [^{11}C]diprenorphine in pituitary was revealed in undernourished restrictive anorexia nervosa patients compared to controls.[40] This latter study was a typical example suggesting that a focus on the quantification of ORs and especially KORs in pituitary could bring rapid and important information in PET imaging of neurologic diseases, while avoiding the problems of BBB permeability and subsequent low brain uptake throughout cerebral sub-structures. In this regard, [^{11}C]RTI-97 with its high pituitary labeling and its unambiguous KOR specificity, would remain a valuable radiotracer for at least preliminary investigation by preclinical PET imaging.

ASSOCIATED CONTENT

Supporting Information

The Supporting Information is available free of charge on the ACS Publications website.

Experimental details, and HPLC analyses (PDF)

AUTHOR INFORMATION

Corresponding Author

* Cécile Perrio - Normandie Univ, UNICAEN, CEA, CNRS, UMR 6030, LDM-TEP, Cyceron, Boulevard Henri Becquerel, 14000 Caen, France; Email: perrio@cyceron.fr

Author Contributions

The manuscript was written through contributions of all authors. All authors have given approval to the final version of the manuscript.

Notes

The authors declare no competing financial interest.

ACKNOWLEDGMENT

The authors thank Région Normandie, CNRS, CEA, Labex IRON (ANR-11-LABX-0018-01) and FR3038 INC3M. They are grateful to the cyclotron operators Mr Olivier Tirel and Mr Jérôme Delamare for production of carbon-11, and to Mrs Martine Dhilly and Mr Laurent Chazalviel from biology laboratory.

REFERENCES

(1) Van't Veer, A.; Carlezon Jr, W. A. Role of kappa-opioid receptors in stress and anxiety-related behavior. *Psychopharmacology* **2013**, *229*, 435-452.

(2) Browne, C. A.; Lucki, I. Targeting opioid dysregulation in depression for the development of novel therapeutics. *Pharmacol. Ther*. **2019**, *201*, 51-76.

(3) Lalanne, L.; Ayranci, G.; Kieffer, B. L.; Lutz, P.-E. The kappa opioid receptor: from addiction to depression, and back. *Front. Psychiatry* **2014**, *5*, 170 (17 pages).

(4) Tejeda, H. A.; Shippenberg, T. S.; Henriksson, R. The dynorphin/k-opioid receptor system and its role in psychiatric disorders. *Cell Mol. Life Sci*. **2012**, *69*, 857-896.

(5) Feng, Y.; He, X.; Yang, Y.; Chao, D.; Lazarus, L. H.; Xia, Y. Current Research on Opioid Receptor Function. *Curr Drug Targets* **2012**, *13*, 230-246.

(6) Le Merrer, J.; Becker, J. A. J.; Befort, K.; Kieffer, B. L. Reward processing by the opioid system in the brain. *Physiol. Rev*. **2009**, *89*, 1379-1412.

(7) Thomas, J. B.; Atkinson, R. N.; Rothman, R. B.; Fix, S. E.; Mascarella, S. W.; Vinson, N. A.; Xu, H.; Dersch, C. M.; Lu, Y.-F.; Cantrell, B.E.; Zimmerman, D. M.; Carroll, F.I. Identification of the first trans-(3R,4R)-dimethyl-4-(3-hydroxyphenyl)piperidine derivative to possess highly potent and selective opioid K receptor antagonist activity. *J. Med. Chem*. **2001**, *44*, 2687-2690.

(8) Beardsley, P. M.; Howard, J. L.; Shelton, K. L, Carroll, F. I. Differential effects of the novel kappa opioid receptor antagonist, JDTic, on reinstatement of cocaine-seeking induced by footshock stressors vs cocaine primes and its antidepressant-like effects in rats. *Psychopharmacology* **2005**, *183*, 118-126.

(9) Carroll, F. I.; Harris, L. S.; Aceto, M. D. Effects of JDTic, a selective κ-opioid receptor antagonist, on the development and expression of physical dependence on morphine using a rat continuous-infusion model. *Eur. J. Pharmacol*. **2005**, *524*, 89-94.

(10) Jackson, K. J.; Carroll, F. I.; Negus, S. S.; Damaj, M. I. Effect of the selective kappa-opioid receptor antagonist JDTic on nicotine antinociception, reward, and withdrawal in the mouse. *Psychopharmacology* **2010**, *210*, 285-294.

(11) Schank, J. R.; Goldstein, A. L.; Rowe, K. E.; King, C. E.; Marusich, J. A.; Wiley, J. L.; Carroll, F. I.; Thorsell, A.; Heilig M. The kappa opioid receptor antagonist JDTic attenuates alcohol seeking and withdrawal anxiety. *Addiction Biol.* **2012**, *17*, 634-647.

(12) Cumming, P.; Marton, J.; Lilius, T. O.; Olberg, D. E.; Rominger, A. A survey of molecular imaging of opioid receptors. *Molecules* **2019**, *24*, 4190 (35 pages).

(13) Kaur, T.; Wiesner, N.; Kilbourn, M. R.; Scott, P. J. H. Classics in neuroimaging: shedding light on opioid receptors with positron emission tomography imaging. *ACS Chem. Neurosci.* **2020**, *11*, 2906-2914.

(14) Naganawa, M.; Jacobsen, L. K.; Zheng, M.-Q.; Lin, S.-F.; Banerjee, A.; Byon, W.; Weinzimmer, D.; Tomasi, G.; Nabulsi, N.; Grimwood, S.; Badura, L. L.; Carson, R. E.; McCarthy, T. J.; Huang, Y. Evaluation of the agonist PET radioligand [^{11}C]GR103545 to image kappa opioid receptor in humans: kinetic model selection, test-retest reproducibility and receptor occupancy by the antagonist PF-04455242. *Neuroimage* **2014**, *99*, 69-79.

(15) Martinez, D.; Slifstein, M.; Matuskey, D.; Nabulsi, N.; Zheng, M.-Q.; Lin, S.-F.; Ropchan, J.; Urban, N.; Grassetti, A.; Chang, D.; Salling, M.; Foltin, R.; Carson, R. E.; Huang, Y.. Kappa-opioid receptors, dynorphin, and cocaine addiction: a positron emission tomography study. *Neuropsychopharmacology* **2019**, *44*, 1720-1727.

(16) Li, S.; Zheng, M.-Q.; Naganawa, M.; Kim, S.; Gao, H.; Kapinos, M.; Labaree, D.; Huang, Y. Development and in vivo evaluation of a κ-opioid receptor agonist as a PET radiotracer with superior imaging characteristics. *J. Nucl. Med*. **2019**, *60*, 1023-1030.

(17) Matuskey, D.; Dias, M.; Naganawa, M.; Pittman, B.; Henry, S.; Li, S.; Gao, H.; Ropchan, J.; Nabulsi, N.; Carson, R. E.; Huang, Y. Social status and demographic effects of the kappa opioid receptor: a PET imaging study with a novel agonist radiotracer in healthy volunteers. *Neuropsychopharmacology* **2019**, *44*, 1714-1719.

(18) Naganawa, M.; Li, S.; Nabulsi, N.; Lin, S.-F.; Labaree, D.; Ropchan, J.; Gao, H.; Mei, M.; Henry, S.; Matuskey, D.; Carson, R. E.; Huang, Y. Kinetic modeling and test-retest reproducibility of ^{11}C-EKAP and ^{11}CFEKAP, novel agonist radiotracers for PET imaging of the kappa opioid receptor in humans. *J. Nucl. Med*. **2020**, *61*, 1636-1642.

(19) Zheng, M.-Q.; Nabulsi, N.; Kim, S. J.; Tomasi, G.; Lin, S.-F.; Mitch, C.; Quimby, S.; Barth, V.; Rash, K.; Masters, J.; Navarro, A.; Seest, E.; Morris, E. D.; Carson, R. E.; Huang, Y. Synthesis and Evaluation of ^{11}C-LY2795050 as a k-Opioid Receptor Antagonist Radiotracer for PET Imaging. *J. Nucl. Med*. **2013**, *54*, 455-463.

(20) Naganawa, M.; Zheng, M.-Q.; Nabulsi, N.; Tomasi, G.; Henry, S.; Lin, S.-F.; Ropchan, J.; Labaree, D.; Tauscher, J.;

Neumeister, A.; Carson, R. E.; Huang, Y. Kinetic modeling of ^{11}C-LY2795050, a novel antagonist radiotracer for PET imaging of the kappa opioid receptor in humans. *J. Cereb. Blood Flo*w Metab. **2014**, *34*, 1818-1825.

(21) Vijay, A.; Cavallo, D.; Goldberg, A.; de Laat, B.; Nabulsi, N.; Huang, Y.; Krishnan-Sarin, S.; Morris, E. D. PET imaging reveals lower kappa opioid receptor availability in alcoholics but no effect of age. *Neuropsychopharmacology* **2018**, *43*, 2539-2547.

(22) Naganawa, M.; Dickinson, G. L.; Zheng, M.-Q.; Henry, S.; Vandenhende, F.; Witcher, J.; Bell, R.; Nabulsi, N.; Lin, S.-F.; Ropchan, J.; Neumeister, A.; Ranganathan, M.; Tauscher, J.; Huang, Y.; Carson, R. E. Receptor occupancy of the κ-opioid antagonist LY2456302 measured with positron emission tomography and the novel radiotracer ^{11}C-LY2795050. *J. Pharmacol. Exp. Ther*. **2016**, *356*, 260-266.

(23) Naganawa, M.; Zheng, M.-Q.; Henry, S.; Nabulsi, N.; Lin, S.-F.; Ropchan, J.; Labaree, D.; Najafzadeh, S.; Kapinos, M.; Tauscher, J.; Neumeister, A.; Carson, R. E.; Huang, Y. Test-retest reproducibility of binding parameters in humans with ^{11}C-LY2795050, an antagonist PET radiotracer for the kappa opioid receptor. *J. Nucl. Med*. **2015**, *56*, 243-248.

(24) Yang, L.; Brooks, A. F.; Makaravage, K. J.; Zhang, H.; Sanford, M. S.; Scott, P. J. H.; Shao, X. Radiosynthesis of [^{11}C]LY2795050 for preclinical and clinical PET imaging using Cu(II)-mediated cyanation. *ACS Med. Chem. Lett.* **2018**, *9*, 1274-1279.

(25) Li, S.; Cai, Z.; Zheng, M.-Q.; Holden, D.; Naganawa, M.; Lin, S.-F.; Ropchan, J.; Labaree, D.; Kapinos, M.; Lara-Jaime, T. A. Navarro, Y. Huang, Novel ^{18}F-labeled κ-opioid receptor antagonist as PET radiotracer: synthesis and in vivo evaluation of ^{18}F-LY2459989 in nonhuman primates. *J. Nucl. Med*. **2018**, *59*, 140-146.

(26) Cai, Z.; Li, S.; Pracitto, R.; Navarro, A.; Shirali, A.; Ropchan, J.; Huang, Y. Fluorine-18-labeled antagonist for PET imaging of kappa opioid receptors. *ACS Chem. Neurosci*. **2017**, *8*, 12-16.

(27) Tangherlini, G.; Börgel, F.; Schepmann, D.; Slocu, S.; Che, T.; Wagner, S.; Schwegmann, K.; Hermann, S.; Mykicki, N.; Loser, K.; Wünsch, B. Synthesis and pharmacological evaluation of fluorinated quinoxaline-based κ-opioid receptor (KOR) agonists designed for PET studies. *ChemMedChem* **2020**, *15*, 1834-1853.

(28) Poisnel, G.; Oueslati, F.; Dhilly, M.; Delamare, J.; Perrio, C.; Debruyne, D.; Barré, L. [^{11}C]-MeJDTic: a novel radioligand for κ-opioid receptor positron emission tomography imaging. *Nucl. Med. Biol*. **2008**, *35*, 561-569.

(29) Schmitt, S.; Delamare, J.; Tirel, O.; Fillesoye, F.; Dhilly, M.; Perrio, C. N-[^{18}F]-FluoropropylJDTic for κ-opioid receptor PET imaging: Radiosynthesis, pre-clinical evaluation, and metabolic investigation in comparison with parent JDTic. *Nucl. Med. Biol*. **2017**, *44*, 50-61.

(30) Thomas, J. B.; Atkinson, R. N.; Vinson, N. A.; Catanzaro, J. L.; Perretta, C. L.; Fix, S. E.; Mascarella, S. W.; Rothman, R. B.; Xu, H.; Dersch, C. M.; Cantrell, B. E.; Zimmerman, D. M.; Carroll, F. I. Identification of (3R)-7-hydroxy-N-((1S)-1-{[(3R,4R)-4-(3-hydroxyphenyl)- 3,4-dimethyl-1-piperidinyl]methyl}-2-methylpropyl)-1,2,3,4-tetrahydro- 3-isoquinolinecarboxamide as a novel potent and selective opioid κ receptor antagonist. *J. Med. Chem*. **2003**, *46*, 3127-3137.

(31) Owens, S. M.; Pollard, G. T.; Howard, J. L.; Fennell, T. R.; Snyder, R. W.; Carroll, F. I. Pharmacodynamic relationships between duration of action of JDTic-like kappa-opioid receptor antagonists and their brain and plasma pharmacokinetics in rats. *ACS Chem. Neurosci*. **2016**, *7*, 1737-1745.

(32) Munro, T. A.; Berry, L. M.; Van't Veer, A.; Béguin, C.; Carroll, F. I.; Zhao, Z.; Carlezon Jr, W. A.; Cohen, B. M. Long-acting κ opioid antagonists nor-BNI, GNTI and JDTic: pharmacokinetics in mice and lipophilicity. *BMC Pharmacology* **2012**, *12*, 5 (18 pages).

(33) Mansour, A.; Fox, C. A.; Akil, H.; Watson, S. J. Opioid-receptor mRNA expression in the rat CNS: anatomical and functional implications. *Trends Neurosci*. **1995**, 18, 22-29.

(34) Zukin, R. S.; Eghbali, M.; Olive, D.; Unterwald, E. M.; Tempel, A. Characterization and visualization of rat and guinea pig brain κ opioid receptors: Evidence for κ_1 and κ_2 opioid receptors. *Proc. Natl. Acad. Sci. USA* **1988**, *85*, 4061-4065.

(35) Placzek, M. S.; Schroeder, F. A.; Che, T.; Wey, H.-Y.; Neelamegam, R.; Wang, C.; Roth, B. L.; Hooker, J. M. Discrepancies in Kappa Opioid Agonist Binding Revealed through PET Imaging. *ACS Chem. Neurosci*. **2019**, *10*, 384-395.

(36) Zhao, B.-G.; Chapman, C.; Bicknell, R. J. Functional c-opioid receptors on oxytocin and vasopressin nerve terminals isolated from the rat neurohypophysis. *Brain Res*. **1988**, *462*, 62-66.

(37) Fjalland, B.; Christensen, J. D. k-Opioid receptor agonists differentially affect the release of neurohypophysial hormones. *Pharmacology & Toxicol*ogy **1990**, *66*, 176-178.

(38) Mansour, A.; Burke, S.; Pavlic, R. J.; Akil, H.; Watson, S. J. Immunohistochemical localization of the cloned κ_1 receptor in the rat CNS and pituitary. *Neurosci*. **1996**, *71*, 671-690.

(39) Mc Lean, S.; Rice, K. C.; Lessor, R.; Rothman, R. B. [^{3}H]Cyclofoxy, a ligand suitable for positron emission tomography, labels mu and kappa opioid receptors. *Neuropeptides* **1987**, *10*, 235-239.

(40) Galusca, B.; Traverse, B.; Costes, N.; Massoubre, C.; Le bars, D.; Estour, B.; Germain, N.; Redouté, J. Decreased cerebral opioid receptors availability related to hormonal and psychometric profile in restrictive-type anorexia nervosa. *Psychoneuroendocrinology* **2020**, *118*, 104711 (9 pages).

Table of Contents